Synthesis and Study of an *N,N*-Disubstituted 4-[(4-Aminophenyl)diazenyl]benzaldehyde

by **Long-Li Lai***, **Chia-Husan Ho**, **Yu-Jen Lin**, and **Eshin Wang**

Department of Applied Chemistry, National Chi Nan University, Puli, Taiwan 545, R.O.C.
(Phone: 886-49-2910960 4975; fax: 886-49-2917956; e-mail: lilai@ncnu.edu.tw.)

and **Yi-Hung Liu** and **Yu Wang**

Instrumentation Center and Department of Chemistry, National Taiwan University, Taipei, Taiwan 106, R.O.C.

and **Yang-Chu Lin** and **Kung-Lung Cheng**

Union Chemical Laboratory, Industrial Research Institute Hsinchu, Taiwan 300, R.O.C.

An *N,N*-disubstituted 4-[(4-aminophenyl)diazenyl]benzaldehyde ('azo dye') with nematic phase was synthesized by reaction of the phenylpiperazine derivative with the formylbenzenediazonium salt. The salt was prepared by a simplified reaction of poly(aminobenzaldehyde) with $NaNO_2$ in the presence of HBF_4. The azo dye was further studied by crystallography. On the basis of molecular stacking identified from crystallography, the molecular modeling was carried out to explore the molecular interactions, and it was found that the attraction of two coplanar molecules with side-to-side contact is favored, and a nematic phase is thus formed during the thermal process.

1. Introduction. – Azo dye molecules have recently attracted a lot of attention in both academia and industry [1][2]. For example, a dichroic dye is dissolved in a liquid crystal to give better reflectance of the polarizer [3]. Furthermore, azo dyes have a reasonable dichroic ratio and are suitable materials for the lower-power-consumption reflective liquid-crystal devices. The three-layered guest-host (G-H) system of the dichroic dye with subtractive color mixing of yellow, magenta, and cyan are expected to be used for developing the full-color reflective displays [4]. Previously, we have successfully synthesized several azo-dye materials of type **1** [5], which show smectic phases. However, the nematic liquid crystals are more valuable in practice, as they possess lower viscosity and faster response under applied electrical switching. Therefore, we designed and synthesized a nematic azo dye containing a CHO function. Such a material is useful for further synthesizing the chiral derivatives [6] that are important in developing the ferroelectric and antiferroelectric displays [7]. To

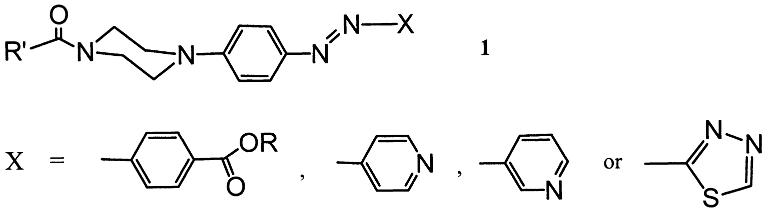

1

understand the molecular stacking of the nematic liquid crystals, the azo dye was studied by single-crystal structure determination. Based on the molecular arrangement identified from crystallography, molecular modeling was further used to investigate the interaction between molecules. A possible model of forming a nematic phase for the azo dye is thus raised because of the successful strategy of combining crystallography and simple molecular modeling. Here, we report our preliminary results.

Results and Discussion. – Compound **2** was prepared by reaction of 1-phenylpiperazine with octanoyl chloride in CH_2Cl_2 in the presence of Et_3N in an almost quantitative yield. The *N*,*N*-disubstituted 4-[(4-aminophenyl)diazenyl]benzaldehyde **4** was synthesized by reaction of compound **2** with diazonium salt **3** according to the *Scheme*. Although the corresponding salt can be synthesized from freshly prepared 4-aminobenzaldehyde [8], the storage of the salt precursor is a problem, as it gradually loses water during the storage. We thus simplified the salt preparation by hydrolyzing the commercially available poly(4-aminobenzaldehyde) in hot tetrafluoroboric acid and then allowing the resulting ammonium benzaldehyde to react with 1.5 equivalents of $NaNO_2$ at 0° (*Scheme*).

Scheme

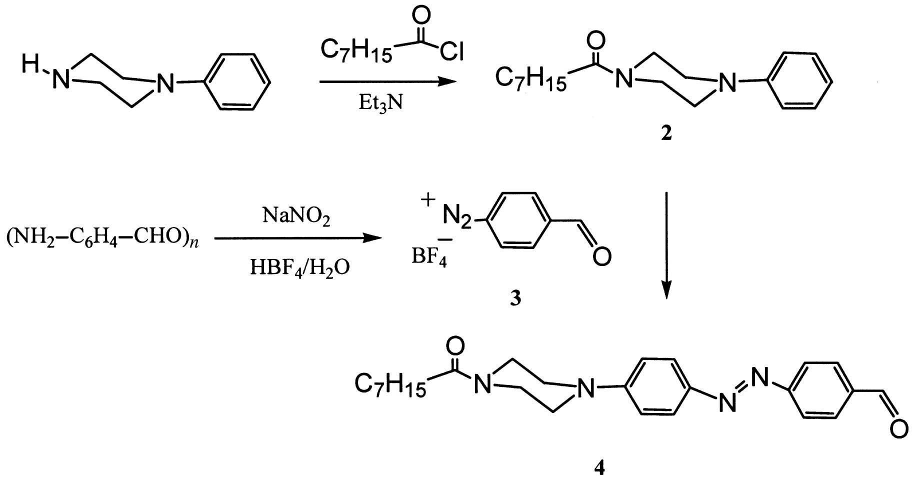

A nematic phase of compound **4** was characterized by the *Schlieren* texture through polarizing optical microscopy. The nematic phase for compound **4** is from 125.4 to 158.7° in the heating process and 158.3 to 107.0° in the cooling process. The nematic phase of compound **4** was confirmed by the powder X-ray diffraction (XRD) study. As there is no layer structure in the range of the nematic phase for the liquid crystals, no reflection was observed in the small angle area for compound **4** from the XRD study.

To understand the molecular stacking of the molecules in the solid state, compound **4** was studied by single-crystal structure determination. The packing diagram for the intermolecular interaction of compound **4** in the solid state is shown in *Figs. 1,a* and *b*. In a vertical layer (for example *A* layer in *Fig. 1,a*), the first and the third molecules are regularly arranged by face-to-face with the head-to-head or tail-to-tail arrangement, and the second molecule is horizontally inserted at one of the ends. On further consideration of the arrangement of compound **4** from the view along the O–b direction in *Fig. 2,a*, molecules in different vertical layers (for example *A*, *B*, and *C* layers) are co-planar side-to-side to each other, as demonstrated in *Fig. 1,b*.

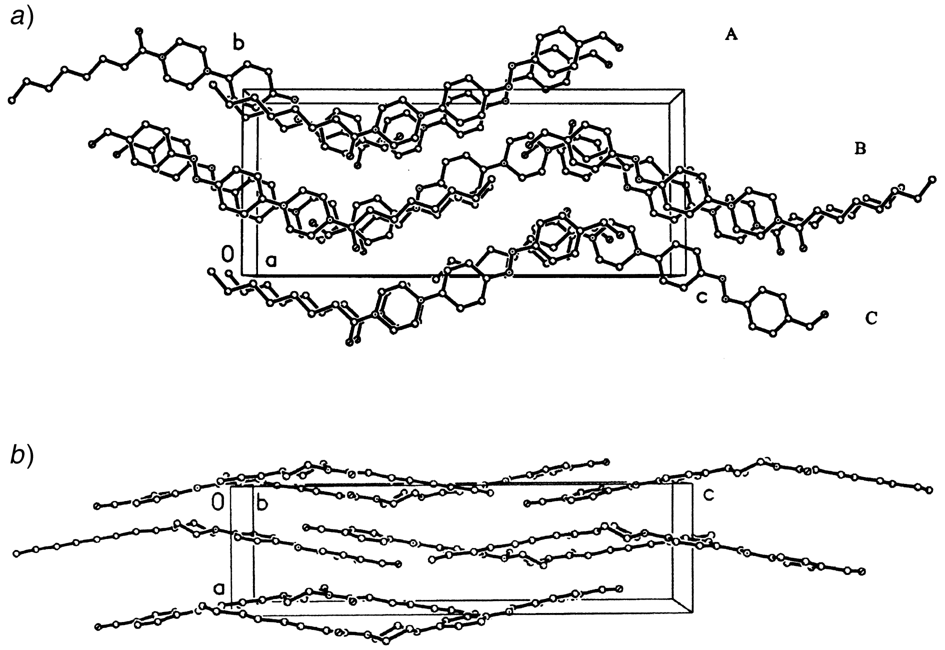

Fig. 1. a) *The packing diagram of compound 4 in a view down the a-axis, H-atoms were omitted for clarity.* b) *The packing diagram of compound 4 in a view down the b-axis, H-atoms were omitted for clarity.*

By the resulting crystallographic data, we calculated the molecular interaction between two representing molecules of **4**, which are parallel to each other by a face-to-face arrangement in the same vertical layer or co-planar to each other by side-to-side arrangement in different vertical layers. Although the calculation results under such conditions are more related to real molecules in the gas phase, we deem that these results may be reasonably applied to the solid state, as the intrinsically attractive and repulsive properties for molecules should remain consistent in gas, liquid, and solid states. Therefore, the conformation of a single molecule of compound **4** was first optimized by performing a geometry calculation in mechanics with augmented MM3 parameters and further refined by calculating the optimized geometry by MOPAC with PM3 parameters. Based on the arrangement in *Fig. 1,a*, two kinds of the two-molecular system shown in *Figs. 2* and *3* were defined preceeding the molecular modeling. In the system of *Fig. 2*, a molecule in one vertical layer is coplanar to another molecule in another vertical layer with side-to-side and head-to-tail contact, which is similar to part of the arrangement identified from crystallography (*Fig. 1,a*). The system was then refined by calculating the optimized geometry by MOPAC with PM3 parameters to seek the minimum energy of the system. To clearly estimate the extent of interaction

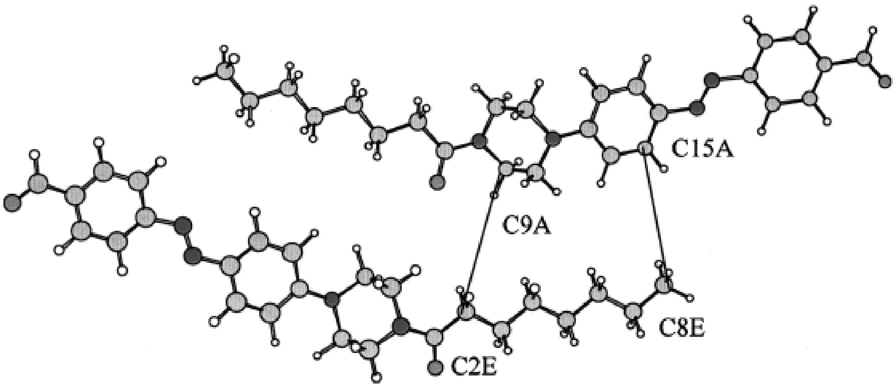

Fig. 2. *The close contact of the two-molecular system of compound* **4** *by side-to-side and head-to-tail arrangement*

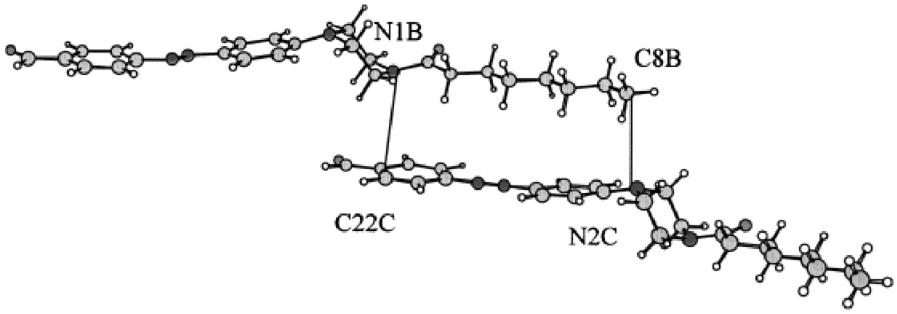

Fig. 3. *The close contact of the two-molecular system of compound* **4** *by face-to-face and head-to-tail arrangement*

between two molecules, after optimizing the two-molecular system, each molecule was further refined by MOPAC with PM3 parameters. Therefore, the corresponding heats of the formation of the two coplanar molecules, shown in *Fig. 2*, were calculated at different distances, and the results were shown in *Table 1*.

Table 1. *The Distances, Lowered Energies, and Other Properties with Respect to* Fig. 2

Heat of formation for the system [kcal/mol]	Heat of formation for individual molecule [kcal/mol]	Distances [Å]		Lowered energy [kcal/mol]
		C(9A)–C(2E)	C(15A)–C(8E)	
– 34.01	– 15.72, – 16.60	5.23	5.18	– 1.70
– 38.22	– 15.75, – 16.62	4.08	3.99	– 5.85
– 41.63	– 15.21, – 15.80	3.84	3.48	– 10.62
– 38.72	– 14.70, – 15.73	3.72	3.42	– 8.29
		4.72[a])	3.93[a])	

[a]) Obtained from X-ray crystal-structure analysis.

The optimum distances of C(9A)–C(2E) and C(15A)–C(8E) according to our calculation are 3.84 and 3.48 Å, respectively, wherein the heat of formation for the two-molecular system is – 41.63 kcal/mol, and the heat of formation for each corresponding molecule is – 15.21 and – 15.80 kcal/mol, respectively. The enthalpy difference is used to investigate whether the two-molecular system shown in *Fig. 2* is more stable than two isolated molecules. Therefore, the sum of the heats of formation for each corresponding molecule was subtracted from the heat of formation of the two-molecular unit and consequently gave an energy difference of – 10.62 kcal/mol. The result indicates that the arrangement in *Fig. 2* is favored on the basis of the stabilization point. If two molecules were moved closer, the energy calculated was lower (– 8.29 kcal/mol), wherein the distances of C(9A)–C(2E) and C(15A)–C(8E) were calculated to be 3.72 and 3.42 Å, respectively. When two molecules were further separated, the calculated energy was also lower (– 5.85 kcal/mol), wherein the distances of C(9A)–C(2E) and C(15A)–C(8E) were calculated to be 4.08 and 3.99 Å, respectively. We thus suggest that the optimum location of molecules shown in *Fig. 2* is as previously described, wherein the distances of C(9A)–C(2E) and C(15A)–C(8E) are in the range of 3.72–4.08 and 3.42–3.99 Å, respectively. When two molecules are moved closer together, the repulsive force between the molecules will increase. The attractive force between two molecules will decrease when the molecules are further separated. As the conformation of the individual molecule in *Fig. 2* slightly changes during the optimization of the two-molecular system, the heat of formation for one molecule may be different from another. However, the variation is not significant and is *ca.* 1 kcal/mol (*Table 1*).

In another system as shown in *Fig. 3*, two molecules in the same vertical layer are orientated face-to-face together with head-to-tail arrangement, which is also similar to part of the arrangement identified from crystallography (*Fig. 1,a*). The interaction of the system was also simulated in a similar manner. The energy between the molecules at the optimized distances is only lowered by *ca.* – 0.01 kcal/mol (*Table 2*). Therefore, we assume that the attraction between the molecules in the same vertical layer, which are in a face-to-face together with head-to-tail arrangement, can be neglected. During the thermal process, two molecules in the same vertical layer of *Fig. 3* dissociates easily, but two co-planar molecules of *Fig. 2* remain as a stable unit for forming the nematic phase during the thermal process. According to the calculation results shown in *Table 1*, the stabilization energy of the two-molecular system shown in *Fig. 2* at optimum distance is 10.62 kcal/mol and rather large when compared with *Van der Waals* forces (1–5 kcal/mol) [9]. Also, the optimum distance between two molecules is smaller than the corresponding distance obtained from crystallography (*Table 1*). This may result from the simplicity of our calculation model. Owing to the limitation of the calculation program and the size of the molecule (63 atoms in compound **4**), the interaction of only two molecules is calculated. The more molecules are involved to calculate their interaction, the more accurate results should be obtained. When the distances of C(9A)–C(2E) and C(15A)–C(8E) are fixed and close to the optimum distances obtained from crystallography (4.72 and 3.93 Å, resp.), the stabilization according to our present calculation should be greater than 1.74 but less than 5.85 kcal/mol, which is consistent with *Van der Waals* forces of the molecules (1–5 kcal/mol). Additionally, the calculation results clearly demonstrate that two coplanar molecules in a side-to-side together with head-to-tail arrangement form a stable unit, and the mesogenic phase during the thermal process is thus formed because of the attractive forces between molecules. On the other hand, two molecules in the same vertical layer by face-to-face together with head-to-tail arrangement are not attracted to each other, and will easily disassociate during the thermal process.

Table 2. *The Distances, Lowered Energies, and Other Properties with Respect to* Fig. 3

Heat of formation for the system [kcal/mol]	Heat of formation for individual molecule [kcal/mol]	Distances [Å]		Lowered energy [kcal/mol]
		N(1B)–C(22C)	C(8B)–N(2C)	
– 32.06	– 15.60, – 16.49	5.02	4.99	+ 0.03
– 32.01	– 15.54, – 16.46	4.50	4.49	– 0.01
– 31.65	– 15.54, – 16.46	3.96	3.92	+ 0.35
– 29.43	– 15.06, – 16.52	3.74 3.89[a])	3.60 3.87[a])	+ 2.15

[a]) Obtained from X-ray crystal-structure analysis.

In conclusion, this work presents a convenient synthesis of a nematic azo-dye molecule with a CHO group, which is useful for further synthesis of chiral liquid crystals. The results from the crystallographic study provide the details of the crystal packing in the solid state and the correlative position of the molecules. The calculation of the interaction between molecules is performed on the basis of arrangement identified from crystallography, and the results show that two coplanar molecules in side-to-side together with head-to-tail arrangement are favored during the thermal process on the basis of the stabilization point. Noteworthy is that the successful strategy of combining crystallography and simple molecular modeling to study the details of the molecular interaction provides a useful method in material chemistry.

Experimental Part

General. Chemicals used were available from *ACROS*. IR Spectra: in cm^{-1}; *Bio-Rad*; *Digilab ITS-60*. ^{1}H- and ^{13}C-NMR spectra: *Bruker 200 FT* NMR spectrometer. High-resolution (HR) MS: *VG70-250*; EI, 70 eV). The mesogenic behaviors and phase transitions were characterized by polarizing optical microscopy and differential scanning calorimetry (*Perkin-Elmer DSC 6*). Powder X-ray diffraction (XRD) patterns were obtained from a *Siemens D-5000* X-ray diffractometer equipped with a *TTK 450* temp. controller and Cu radiation with the wavelength of $\lambda = 1.5406$ Å. Semi-empirical calculation was carried out with the CAChe program, which was provided by *Fujitsu* (version 3.2).

Synthesis of 4-{[4-(Octanoylpiperazin-1-yl)phenyl]diazenyl}benzaldehyde (**4**). Poly(4-aminobenzaldehyde) (1.21 g, 10 mmol) was added to HBF_4 (50wt-% in H_2O; 8 ml), which was then diluted with hot H_2O (*ca.* 90°; 7 ml). $NaNO_2$ (1.03 g, 15 mmol) was gradually added at 0°, and the soln. was then kept in the refrigerator overnight. Diazonium salt **3**, which had precipitated, was filtered off, washed with dry Et_2O and then dried to give quant. yield. The phenylpiperazine derivative **2** (2 mmol) was added to salt **3** (2.4 mmol) in AcOH (10 ml), and the soln. was stirred for 2 h at r.t. H_2O (100 ml) was added, and the mixture was extracted with CH_2Cl_2 (2 × 100 ml). The combined extracts were dried (Na_2SO_4), and the solvent was removed at reduced pressure. The residue was chromatographed on silica gel to give **4** (40.8%, 0.342 g), which was characterized as the correct compound by spectroscopy. IR: 2948, 2919, 2847, 2731, 1694, 1643, 1595, 1561, 1542, 1509, 1457, 1428, 1391, 1370. ^{1}H-NMR ($CDCl_3$): 0.85 (*t*, $J = 6.6$, Me); 1.29–1.36 (*m*, 4 CH_2); 1.57–1.66 (*m*, CH_2); 2.33 (*t*, $J = 7.8$, CH_2); 3.40 (br. *s*, 2 CH_2); 3.66 (br. *s*, CH_2); 3.80 (br. *s*, CH_2); 6.95 (*AA′BB′*, $J = 8.8$, 2 arom. H); 7.92 (*AA′BB′*, $J = 8.8$, 2 arom. H); 7.97 (br. *s*, 4 arom. H); 10.05 (*s*, CHO). ^{13}C-NMR ($CDCl_3$): 191.56 (CHO); 171.77 (C=O);

156.31; 153.10; 145.48; 136.52; 130.59; 125.29; 122.78; 114.43; 47.67; 47.44; 44.93; 40.89; 33.20; 31.60; 29.33; 29.00; 25.18; 22.51; 14.00. HR-MS: 420.2526 ($C_{25}H_{32}N_4O_2$; calc. 420.2525).

X-Ray Crystal-Structure Analysis. Crystals of compound **4** were grown from CH_2Cl_2/hexane 1:1 at r.t. Single crystal of suitable quality was mounted on a glass fiber and used for measurement of precise cell constants and intensity-data collection. Diffraction measurement was made on a *Siemens SMART 1K CCD* diffractometer with graphite-monochromated MoK_α radiation ($\lambda = 0.71073$ Å), operated at 150(2) K over the θ range of 1.54–23.26°. No significant decay was observed during the data collection. 2269 Reflections were observed with $I \leq 2\sigma\ (I)$ among the 3188 unique reflections, and 2987 reflections were used in the refinement. Data were processed on a PC with the SHELXTL software package [10]. The structure of **4** was solved by direct methods and refined by full-matrix least square on F^2 value. All non-H-atoms were refined anisotropically. The H-atoms were fixed at calculated positions and refined using a riding model. The final indices were $R1 = 0.0441$, $wR2 = 0.0901$ with goodness-of-fit on $F^2 = 1.000$. Further data: formula: $C_{25}H_{32}N_4O_2$; formula weight: 420.55; crystal size: $0.02 \times 0.10 \times 0.25$ mm^3; unit-cell parameters: $a = 7.4709(7)$, $b = 11.2442(10)$, $c = 26.389(3)$ Å, $\alpha = \beta = \gamma = 90°$; crystal system: orthorhombic; space group: $P2_12_12_1$; $V = 2216.8(4)$ Å^3; cell units: $Z = 4$; calc. density 1.260 g cm^{-3}; linear absorption coefficient 0.081 (μ/cm^{-1}). Crystallographic data for the structure **4** has been deposited with the *Cambridge Crystallographic Data Centre (CCDC)* as supplementary publication No. CCDC-164793. Copies of the data can be obtained, free of charge on application to CCDC, 12 Union Road, Cambridge CB2 1EZ, UK fax: (+44) 1223-336-033; e-mail: deposit@ccdc.cam.ac.uk.

We thank the *National Chi Nan University* and the *National Science Council* (NSC 89-2113-M-260-005) for financial support. The *National Center of High-Performing Computing* and the *Institute of Chemistry*, *Academia Sinica*, are also acknowledged for providing the *Beilstein* database system, as well as the most helpful library service and the XRD apparatus, respectively.

REFERENCES

[1] a) B. L. Feringa, R. A. van Delden, N. Koumura, E. M. Geertsema, *Chem. Rev.* **2000**, *100*, 1789; b) S. Kawata, Y. Kawata, *Chem. Rev.* **2000**, *100*, 1777; c) J. A. Delaire, K. Nakatani, *Chem. Rev.* **2000**, *100*, 1817; d) K. Ichimura, *Chem. Rev.* **2000,** *100,* 1847.

[2] a) C. Ruslim, K. Ichimura, *Chem. Lett.* **1998**, 789; b) D. S. Hermann, P. Rudquist, K. Ichimura, K. Kudo, L. Komitov, S. T. Lagerwall, *Phys. Rev. E.* **1997**, *55*, 2857; c) V. P. Shibaev, S. G. Kostromin, S. A. Ivanov 'in Polymer as Electrooptical and Photooptical Active Media', Ed. by V. P. Shibaev, Berlin, Springer, 1996, pp. 37–110.

[3] a) D. J. Broer, J. Lub, US Patent No. 5506704, 1996; b) C. M. Berke, US Patent No. 4440541, 1982.

[4] a) D. Bauman, *Mol. Cryst. Liq. Cryst.* **1988**, *159*, 197; b) K. Sunohara, K. Naito, M. Tanaka, Y. Naikai, N. Kamiura, K. Taira, 'SID '96 Digest' **1996**, p 103; c) K. Taira, H. Iwanaga, A. Hotta, Y. Nakai, T. Ohtake, K. Sunohara, 'AM-LCD '96' 1996, p. 333; d) M. Tanaka, *FPD Intelligence* **1997**, *4*, 70.

[5] a) L. L. Lai, H.-C. Lin, *Liq. Cryst.* **2000**, *27*, 707; b) L. L. Lai, E. Wang, L. J. Lee, J. J. Chen, D. W. Yang, *Liq. Cryst.* **2001**, *28*, 157; c) L. L. Lai, L. J. Lee, E. Wang, F. Y. Su, *Liq. Cryst.* **2001**, *28*, 381; d) L. L. Lai, L. J. Lee, G. H. Lee, Y. Wang, K. H. Lu, S. J. Lee, *Liq. Cryst.* **2001**, 1513; e) L. L. Lai, E. Wang, *Helv. Chim. Acta* **2001**, *84*, in press.

[6] K. Soai, S. Niwa, *Chem. Rev.* **1992**, *92*, 833.

[7] a) P. Rudqist, J. P. F. Lagerwall, M. Buivydas, F. Gouda, S. T. Lagerwall, N. A. Clark, J. E. Maclennan, R. Shiao, D. A. Coleman, S. Bardon, T. Bellini, D. R. Link, G. Natale, M. A. Glaser, D. M. Walba, M. D. Wand, X. H. Chen, *J. Mater. Chem.* **1999**, *9*, 1257; b) R. Beccherelli, S. J. Elston, *Liq. Cryst.* **1998**, *25*, 573; c) Y. Chen, W. J. Wu, *Liq. Cryst.* **1998**, *25*, 309; d) W. K. Robinson, C. Carboni, P. Kloess, S. P. Perkins, H. J. Coles, *Liq. Cryst.* **1998**, *25*, 301.

[8] a) A. Yasuhara, A. Kasano, T. Sakamoto, *J. Org. Chem.* **1999**, *64*, 2301; b) E. Fritz-Langhals, B. Kunath, *Tetrahedron Lett.* **1998**, *39*, 5955; c) J. S. Cha, J. E. Kim, M. S. Yoon, Y. S. Kim, *Tetrahedron Lett.* **1987**, *28*, 6231.

[9] B. E. Douglas, D. H. McDaniel, J. J. Alexander, 'Concept and Models of Inorganic Chemistry', John Wiley & Sons, 1994, pp 99–102.

[10] G. M. Sheldrick, SHELXTL, Version 5.03, *Siemens Analytical X-Ray Instruments Inc.* Madison, Wisconsin, 1994.

Received June 13, 2001